IEEE Access
Multidisciplinary ⋮ Rapid Review ⋮ Open Access Journal

Received September 16, 2020, accepted September 28, 2020, date of publication October 2, 2020, date of current version October 14, 2020.

Digital Object Identifier 10.1109/ACCESS.2020.3028377

Hexagonal Shaped Near Zero Index (NZI) Metamaterial Based MIMO Antenna for Millimeter-Wave Application

SAMIR SALEM AL-BAWRI[1], (Member, IEEE), MOHAMMAD TARIQUL ISLAM[2], (Senior Member, IEEE), TAYYAB SHABBIR[2], GHULAM MUHAMMAD[3], (Senior Member, IEEE), MD. SHABIUL ISLAM[4], (Senior Member, IEEE), AND HIN YONG WONG[4], (Senior Member, IEEE)

[1]Pusat Sains Angkasa, Institut Perubahan Iklim, Universiti Kebangsaan Malaysia, Bangi 43600, Malaysia
[2]Department of Electrical, Electronic and Systems Engineering, Faculty of Engineering and Built Environment, Universiti Kebangsaan Malaysia (UKM), Bangi 43600, Malaysia
[3]Department of Computer Engineering, College of Computer and Information Sciences, King Saud University, Riyadh 11543, Saudi Arabia
[4]Faculty of Engineering, Multimedia University, Cyberjaya 63100, Malaysia

Corresponding authors: Samir Salem Al-Bawri (s.albawri@gmail.com) and Mohammad Tariqul Islam (tariqul@ukm.edu.my)

This work was supported in part by the Universiti Kebangsaan Malaysia Research Grant under Grant number DIP-2019-010, and in part by the Researchers Supporting Project number (RSP-2020/34), King Saud University, Riyadh, Saudi Arabia. The authors, therefore, acknowledge with thanks to King Saud University for technical and financial support.

ABSTRACT A single-layered multiple-input multiple-output (MIMO) antenna working at 28 GHz loaded with a compact planar-patterned metamaterial (MTM) structures is presented in this paper for millimeter-wave application. A combination of a split square and hexagonal shaped unit cell is designed and investigated with a wide range of effective near-zero index (NZI) of permeability and permittivity, along with a refractive index (NZRI) property. The metamaterial characteristics were examined through the material wave propagation in two main directions at y and x-axis. For wave propagation at the y-axis, it demonstrates mu-near-zero (MNZ) with more than 6 GHz bandwidth, near-zero refractive index (NZRI), and epsilon-near-zero (ENZ) properties. However, it indicates a wide negative range of single mu metamaterial (MNG) from 27.6 to 28.9 GHz frequency span at x-axis wave propagation. A single antenna with 3×3 metamaterial unit cells is proposed to operate at a frequency band (24 – 30) GHz. Furthermore, MIMO antenna with only 4 mm space between antenna elements provides high isolation of more than 24 dB. The measured results show that the MIMO antenna is satisfied with 6 GHz bandwidth, and maximum peak gain of 12.4 dBi. In addition to that, the proposed MIMO antenna loaded with MTM has also shown good performances with high diversity gain (DG > 9.99), envelope correlation coefficient (ECC) lower than 0.0013, channel capacity loss (CCL) < 0.42, total active reflection coefficient (TARC) < -7 dB, total efficiencies of higher than 98%, with an overall antenna size of 52 mm $\times$ 23 mm.

INDEX TERMS Millimeter-wave (mm-wave), antenna array, metamaterial (MTM), high isolation, near-zero index (NZI) metamaterial, envelope correlation coefficient, high gain.

I. INTRODUCTION

Nowadays, the tremendous development of the next millimeter-wave (mm-Wave) fifth-generation (5G) communication technology and antennas have been highly demanded due to meet the call for low latency, higher data rate, low cost, less usage of energy and supported transfer information for a considerable number of subscribers devices that deals with various applications beyond mobile communications and cellular industry [1], [2].

Currently, researches of 5G wireless communication systems are mostly concentrating significantly on the mm-Wave range due to the spectrum resources limitation. Moreover, the 28 GHz frequency band has gained significant attention worldwide due to the ingenious spectrum and larger bandwidth [3]. The system channel capacity can significantly be increased by employing the MIMO technology without increasing the antenna transmitting power and

The associate editor coordinating the review of this manuscript and approving it for publication was Raghvendra Kumar Kumar Chaudhary.

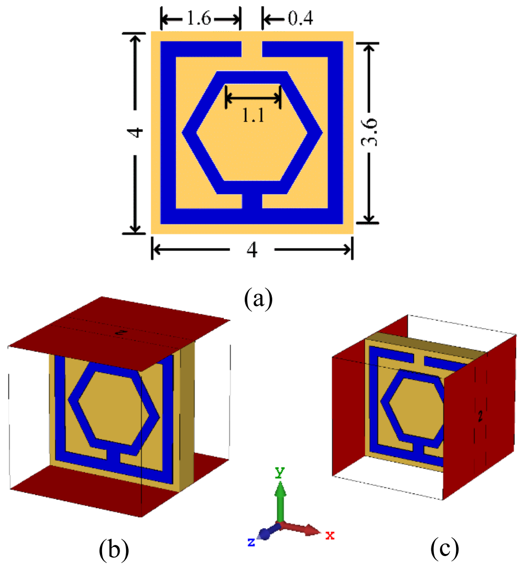

FIGURE 1. MTM unit cell configurations: (a) unit cell geometry, (b) y-axis simulation set up, (c) x-axis simulation set up.

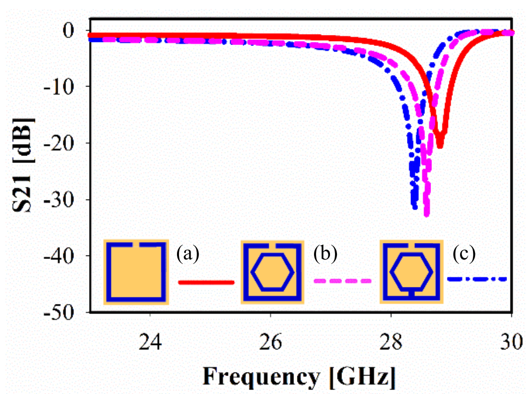

FIGURE 2. Transmission coefficients at y-axis. (a) without inner connector, (b) with inner connector, (c) proposed MTM unit cell.

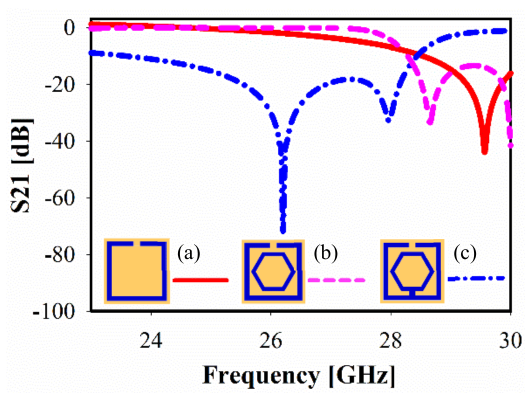

FIGURE 3. Transmission coefficients at x-axis. (a) without inner connector, (b) with inner connector, (c) proposed metamaterial unit cell.

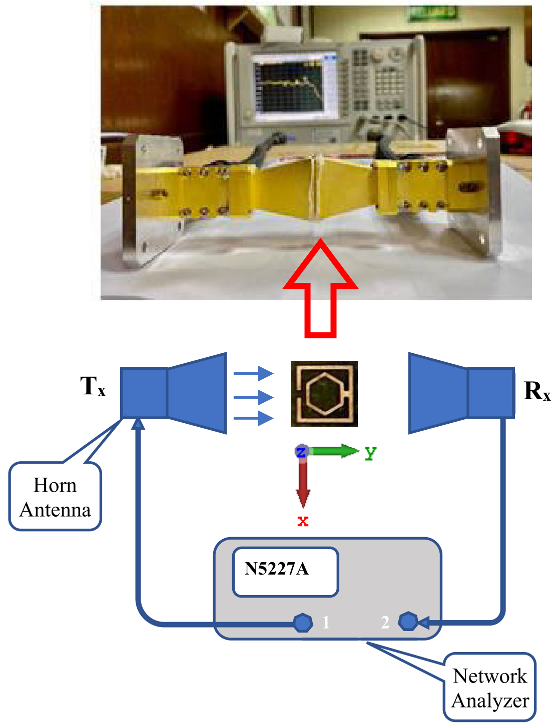

FIGURE 4. Metamaterial experimental setup of the proposed metamaterial structure.

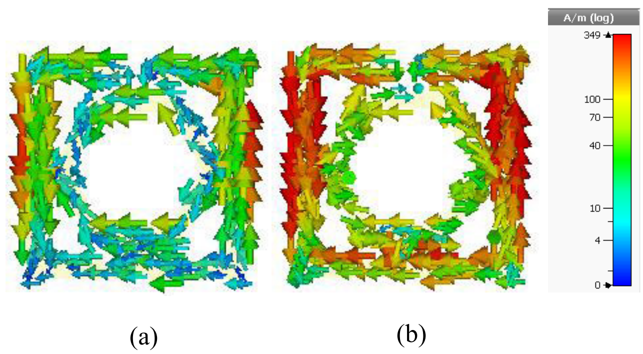

FIGURE 5. MTM unit cell surface current distribution at (a) 27 GHz, (b) 28 GHz.

spectrum resources [4]. Furthermore, MIMO elements should be properly decoupled with a minimum distance from the neighboring elements [5], [6].

However, the main challenge for the researchers is the isolation enhancement between each adjacent elements of designed MIMO as well as miniaturization, whereas the inter-coupling will affect the antenna efficiency and the overall performance of the wireless system. A lot of approaches have been discussed previously in literature to achieve the high isolation between the MIMO antenna elements. These decoupling techniques include hybrid feeding with orthogonal modes, frequency selective surfaces to displace current between elements, parasitic structures at the expense of size and space, metasurface shielding [7]–[11], artificial metamaterials [12], and electronic bandgap (EBG) [13]. Moreover, the enhancement of mutual coupling has been introduced in literature as one of the essential factors in MIMO technology.

Besides, different types of metamaterials are also used to decrease the isolation among the elements of the designed antenna [14], [15]. However, the decoupling techniques mentioned earlier are challenging to implement on miniaturized

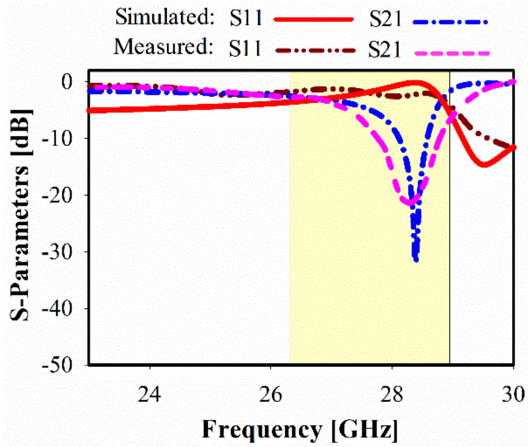

FIGURE 6. Measured and simulated metamaterial S-parameters at the y-axis.

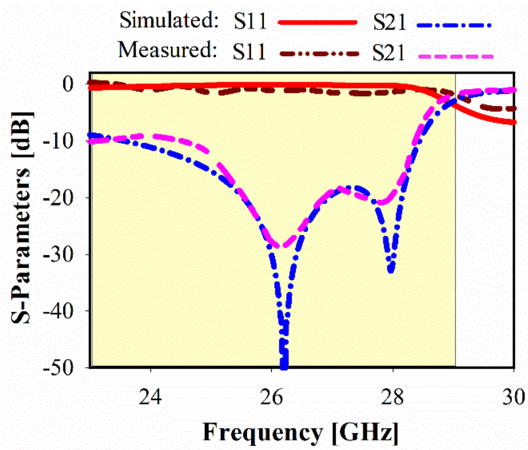

FIGURE 7. Measured and simulated metamaterial S-parameters at the x-axis.

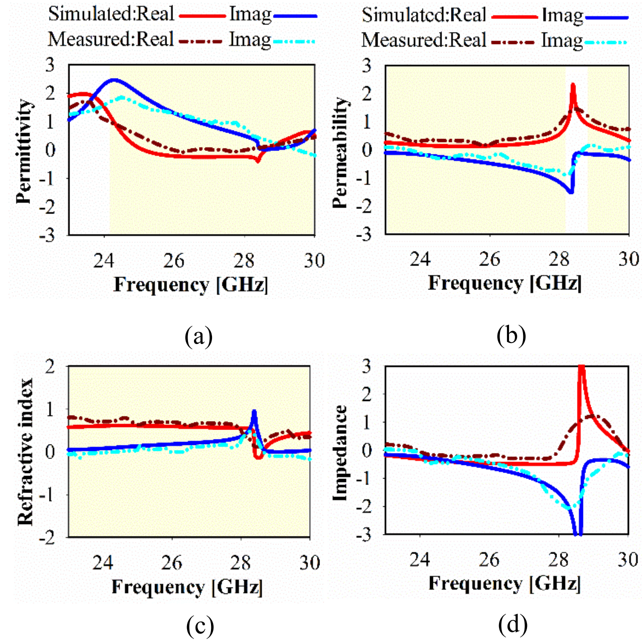

FIGURE 8. MTM measured and simulated results at y-axis: (a) permittivity, (b) permeability, (c) refractive index, (d) impedance.

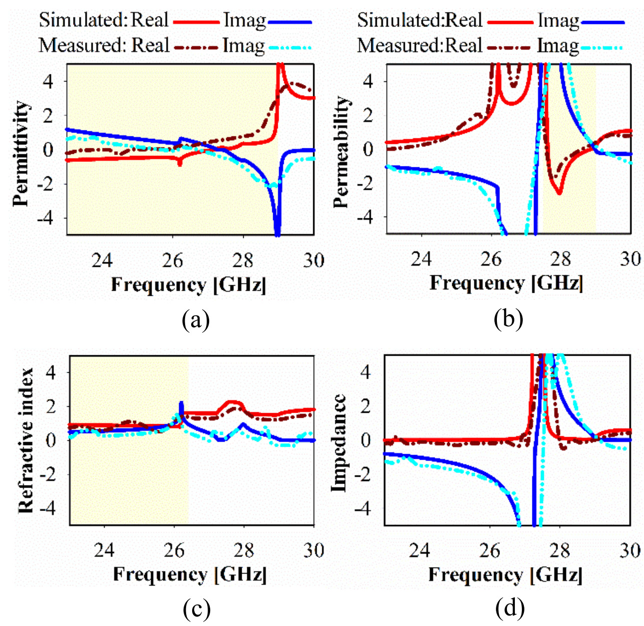

FIGURE 9. MTM measured and simulated results at x-axis (a) permittivity, (b) permeability, (c) refractive index, (d) impedance.

MIMO elements and are challenging to function. Therefore, this paper performs a series of compact split-ring resonators (SRRs) as resonators and to mitigate the coupling between antenna array, unlike conventional Franklin antenna arrays in [16]. Currently, metamaterials with negative (permeability, refractive index and permittivity) characteristics are employed to enhance antenna's bandwidth [17]–[19], [21]. Additionally, a significant increase in the gain, along with excellent radiation, is achieved by employing the metamaterial structure within the antenna design [22]. However, a double negative and NZRI based metamaterial operating in S, C, and X-band are used to improve the antenna performance, i.e., gain, efficiency, radiation characteristics, etc. [23]–[26].

In this paper, a unique metamaterial (MTM) based near-zero property of refractive index, permeability, and permittivity is designed for simultaneous enhancement of the isolation and the overall MIMO antenna system performance. The proposed MTM is loaded and applied as a series of square-hexagonal-shaped of six-element patch radiators elements of MIMO antenna systems. The proposed MTM based MIMO antenna can cover the frequency range from 24 to 30 GHz with a measured bandwidth (BW) of 6 GHz. Unlike conventional isolation reduction techniques, the suggested MTM based method provides high decoupling up to 24 dB between MIMO radiating elements and ECC < 0.0013 with miniaturized array element. Also, to validate the proposed technique, the extracted results from CST microwave studio have been compared with the experimental results, which demonstrate an excellent agreement with each other verifying the properly of the suggested MTM, single antenna, and MIMO antenna.

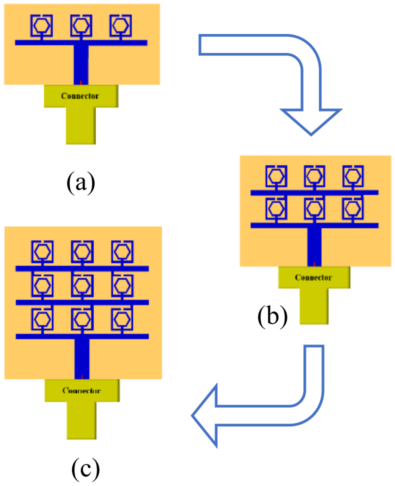

FIGURE 10. Single element antenna step-by-step design.

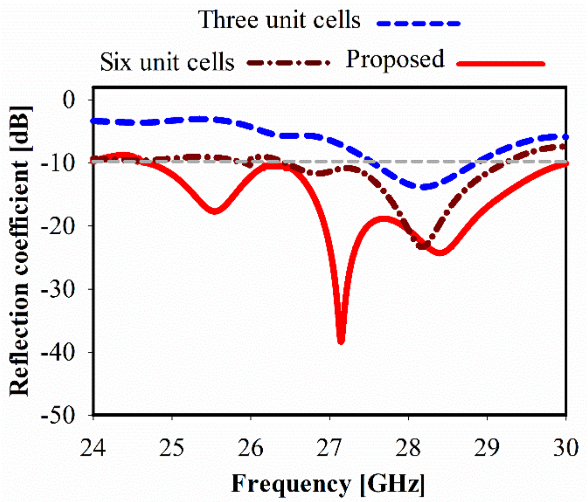

FIGURE 11. Design methodology for different MTM array cells.

II. DESIGN OF METAMATERIAL UNIT CELL

The proposed MTM unit cell schematic view, along with its geometrical design parameters, is illustrated in Fig. 1(a). Each single unit cell consists of a compact square split ring resonator (SSRR) combined with a hexagonal-shaped structure by a 0.3 mm width slab. Low loss Rogers 5880 substrate has been used for MTM unit cell design which has a tiny thickness with 0.79 mm, a loss tangent δ of 0.0009, and 2.2 value of dielectric constant (ε_r).

To verify the unit cell working principle, two simulations setup were applied, as demonstrated in Figs 1(b) and (c) in the y-direction and x-direction, respectively. It represents the simulated electromagnetic wave propagation of the proposed metamaterial design where it was placed between two waveguide ports. The boundary condition including perfect electric conductor (PEC) has been applied to either the x-axis or y-axis, whereas the perfect magnetic (PMC) is applied for the z-axis. It is formed in vertical x-direction on top of the same substrate with a 3 mm distance between every two units. Finite-difference time-domain solver has been used

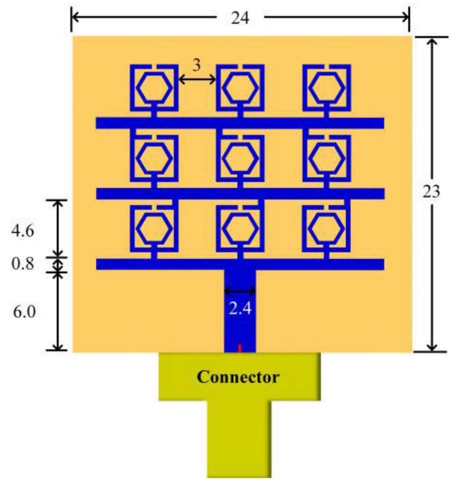

FIGURE 12. The proposed single antenna Geometry (Unit: mm).

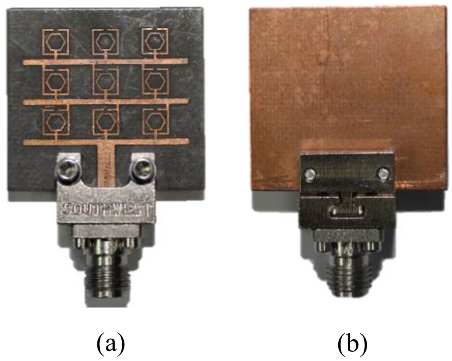

FIGURE 13. Fabricated single antenna prototype (a) top view (b) back view of ground-plane.

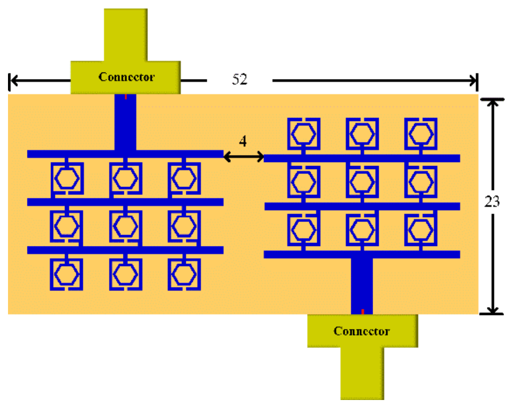

FIGURE 14. 2-D view of the two-port MIMO antenna structure (Unit: mm).

for simulation-based on Computer Simulation Technology (CST).

The proposed MTM unit cell is divided into two metallic rings. The initial outer square ring was split by 0.4 mm on the top arm (see Fig. 2a) prior to including an additional inner hexagonal-shaped conductor. A metallic strip of 0.4 mm width is employed to connect both rings together, as illustrated in Fig. 2(c). The metal strip lines will perform as inductors, whereas capacitive characteristics are achieved

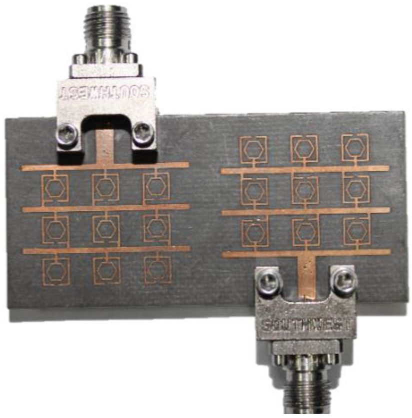

FIGURE 15. Fabricated MTM MIMO antenna prototype.

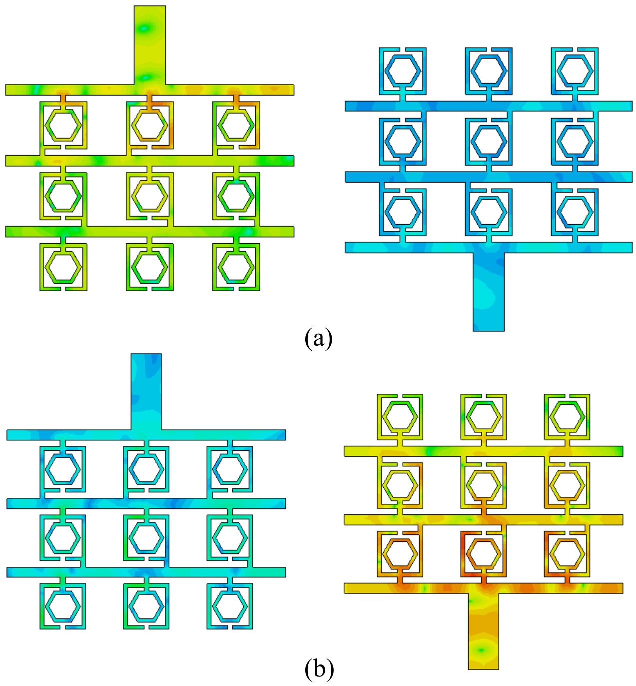

FIGURE 16. Simulated current distribution of the proposed MIMO antenna at (a) 27 GHz, (b) 28 GHz.

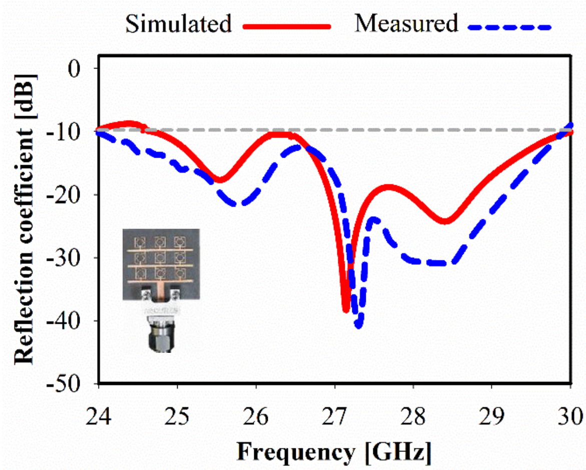

FIGURE 17. Simulated and measured reflection coefficient of the single port antenna array.

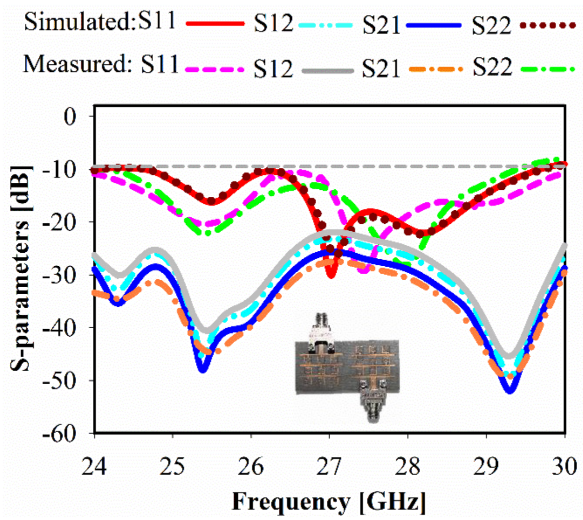

FIGURE 18. Simulated and measured S-parameters of the MIMO antenna.

due to gaps in the outer and inner strip line connectors. Figs. 2 and 3, summarizes the step-by-step MTM unit cell design process at y and x-axis whereas the transmission coefficients indicate the resonance shifted toward the lower frequency band.

Robust method is applied to extract the efficacious metamaterial parameters by using the normal collected incidences data of scattering parameters [22]. Initially, simulations are applied in a frequency range of (23-30 GHz) and analyzed the (S21) and (S11) parameters of the proposed MTM.

The achieved MTM unit cell S-parameters are retrieved by using an Agilent N5227A PNA Network Analyzer attached with waveguides to co-axial adapters. A waveguide SAR-1834031432-KF-S2-DR (18 GHz - 40 GHz) has been utilized for the desired frequency range, whereas the MTM prototype has been placed for measurements between two waveguides in x and y directions as shown in Fig. 4.

III. METAMATERIAL WORKING PRINCIPLE

The surface current distribution at different frequencies is utilized to understand the MTM unit cell behavior, physical work phenomena in the electric and magnetic field regions. The proposed unit cell MTM surface current distributions at 27 GHz and 28 GHz are shown in Figs. 5(a) and 5(b). Arrows represent the surface current distribution while the color represents the density of the surface current. A perceptible surface current is observed at 27 GHz. However, the surface current is more concentrated and intensive on the edge of outer symmetric square-shaped portions. Moreover, the surface current is perturbed in the overall MTM unit cell structure. Although, opposite side directions of the current distribution are observed of MTM-shaped etching strips once the current flows, which is nullifying the current and generates a stopband.

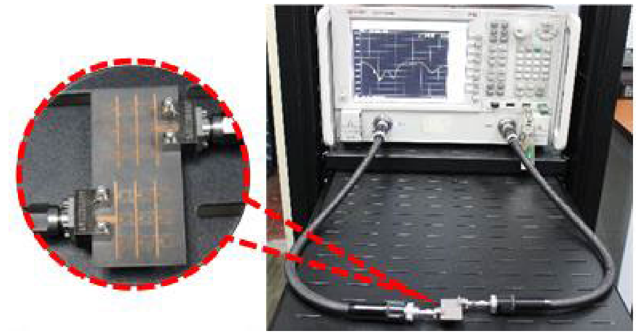

FIGURE 19. Fabricated MIMO antenna S-parameters, measurement setup.

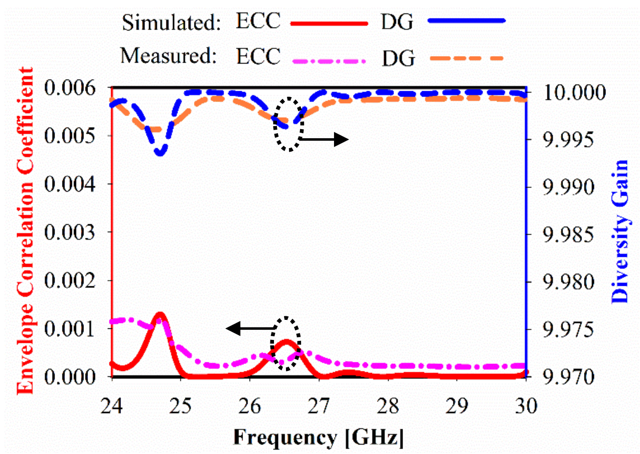

FIGURE 20. Envelope correlation coefficient (ECC) and diversity gain of the proposed MIMO antenna.

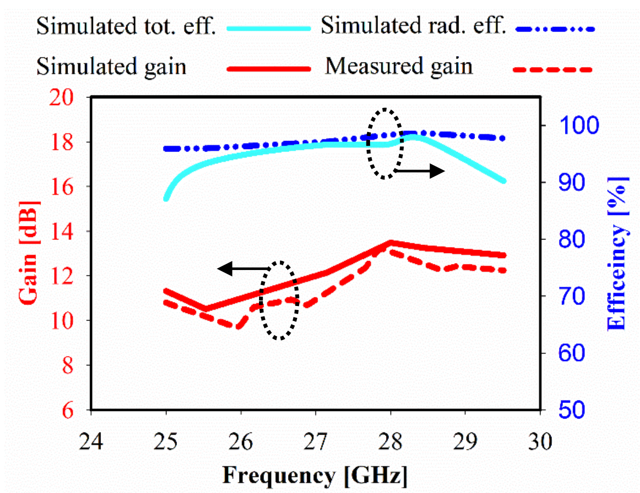

FIGURE 21. Gain and efficiency over the frequency of the proposed MIMO antenna.

The measured and simulated S-parameters (S11 and S21) results of the y-axis and x-axis are displayed in Fig 6 and Fig. 7, respectively. For y-direction, it illustrates that the frequency resonance band at the range of (26.4 – 29.1 GHz) is a part of the Ka-band as well as covering the 5G band. The outer split square-shaped resonator integrated with the inner hexagonal shape is considered as the sufficient cause of the attained stopband operational band. However, for x-direction, a wide stopband resonance is observed above 23 GHz.

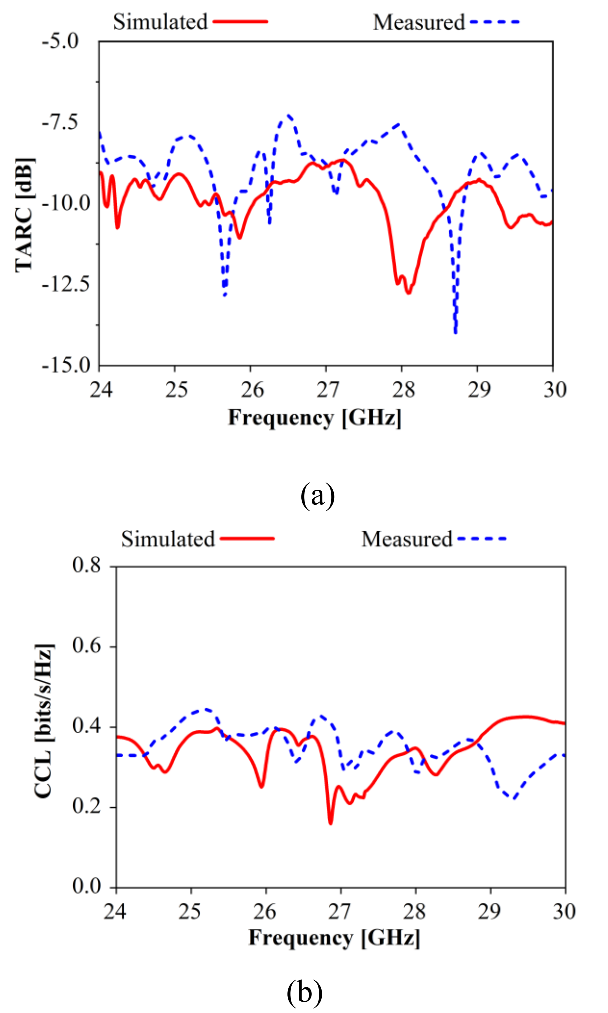

FIGURE 22. MIMO system performance parameters. (a) CCL. (b) TARC.

The metamaterial effective parameters of the selected frequency span are calculated by using a Robust Method [17], [27]. The S-parameters are simulated and optimized using CST, as an electromagnetic full-wave software whose accuracy has been certified. The MTM unit cell is simulated along the y and x directions, with periodic structure boundaries which applied along the z-x and z-y directions, respectively. The resonant property phenomena are accompanied by resonant behavior which mainly results from endeavoring to extract the properties of spatially local material within the desired frequency range.

The proposed metamaterial effective parameters are plotted in Figs. 8 and 9. These parameters include effective imaginary and real values of refractive index, permeability, permittivity, and impedance for different MTM unit cell configurations. In all diagrams, the negative indexed zone for single-negative metamaterial (SNG), Epsilon/Mu near zero (ENZ/MNZ) metamaterial along with NZRI are highlighted with light yellow color.

An extensive real value of NZRI exhibits in the range of (23 – 30 GHz) at y-axis wave propagation, as shown in Fig. 8(c), whereas ENZ and MNZ portions are achieved

TABLE 1. Performance comparisons with the published state of the art.

Ref.	[32]	[33]	[34]	[35]	[36]	[37]	[38]	**This work**
Technique	Vias	Metasurface	Metallic-based slot antenna	Tapered-Fed Antenna	DR-Based Antenna	Mushroom Electromagnetic Band Gap (EBG)	Metallic-Based Slot Antenna	**Metamaterial-Based MIMO Antenna**
No. of Ports	2	2	2	2	2	2	2	**2**
*Size (W × L)	$1.98\ \lambda_0 \times 5.82\ \lambda_0$	- -	$3.89\lambda_0 \times 1.47\lambda_0$	$0.34\lambda_o \times 0.18\lambda_o$	$4.82\lambda_o \times 2.107\lambda_o$	$0.67\lambda_o \times 0.46\lambda_o$	$0.83\lambda_o \times 0.42\lambda_o$	**$4.42\lambda_o \times 1.95\lambda_o$**
BW (GHz) <-10 dB	25.2–27.1	24.2-27.8 36.9-42.8	22.5–50	02.93 –20.00	29.70 – 31.50	02.50 –11.00	03.00 – 30.00	**24.00 –29.90**
Max. Edge to Edge Space (λ_0)	0.11	- -	5.25	0.40	0.28	0.14	- -	**0.36**
Max. Gain, dBi	06.60	10.99	15.00	07.00	07.00	06.00	- -	**13.40**
Rad. Efficiency %	- -	83	84	85	80	80	- -	**98**
Min. Isolation, dB	30	24	20	22	25	15	20	**24**
ECC	0.0020	- -	0.12000	0.01000	0.0020	0.0200	- -	**0.0013**

*Based on the lowest frequency

with 6 GHz and 5.1 GHz bandwidth, respectively, as illustrated in Figs 8(a) and 8(b). A bandwidth of more than 3 GHz is realized with NZRI property in wave propagation of the x-axis, as depicted in Fig. 9 (c). This frequency band can be used for high gain antenna design and electromagnetic cloaking. Moreover, MNZ property exhibits for the frequency span from 27.6 to 28.9 GHz as represented in Fig. 9(b) while the lower band of the KA band is covered using the unique proposed MTM in wave propagation at x-direction.

IV. CONFIGURATION OF THE PROPOSED ANTENNA

Two metamaterial antennas are designed and mounted on the Rogers 5880 substrate with relative permeability, permittivity, thickness, and $\tan\delta$ of 1, 2.2, 0.79 mm, and 0.0009, respectively. The detailed configuration approach of the suggested antennas is demonstrated as follows.

A. SINGLE ANTENNA

The metamaterial-based antenna design is a novel method to achieve better impedance matching in the compact unit cell configuration. The evaluation process of the MTM based single antenna is illustrated in Figs. 10 and 11. Initially, a cluster of three MTM cells is arranged horizontally and attached to the microstrip line. By using a 3-cell array, an impedance matching over 27.5 GHz to 28.8 GHz frequency band is achieved, not covering the entire mm-Wave frequency band. The proposed antenna design bandwidth is improved by using the 6-cells MTM array configuration. The array elements are inter-linked through metallic strips. A wider bandwidth from 26.5 GHz to 29 GHz is achieved by using this array configuration. This array is also not covering the intended frequency range. Finally, a 9-cells array configuration is

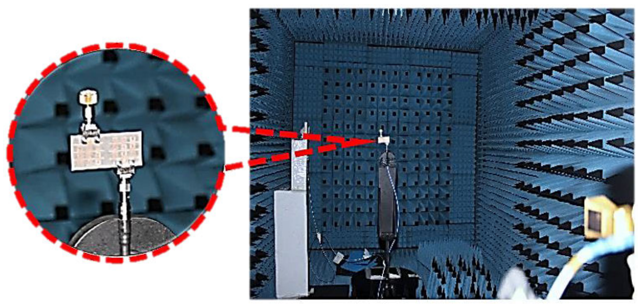

FIGURE 23. Measurement setup of the radiation pattern.

applied to achieve a wider bandwidth with S11 < -10 dB in 24 GHz to 30 GHz frequency band. The single antenna element design procedure and the noticeable effect on the reflection coefficient are illustrated in Figs. 10 and 11. During the single antenna design process main goal is to achieve better matching in 24 GHz to 30 GHz frequency band.

Fig. 12 demonstrates the geometry configuration of the simulated single-port antenna. A series of 3×3 compact MTM unit cell elements are presented, whereas each structure forming a hexagonal radiator. Moreover, the proposed antenna is fed by a transmission line with a length and width of 6 mm, and 2.4 mm, respectively, as well as 50 Ω impedance of feedline. It is followed by E- shaped divider, this junction has three thin arms with a 0.4 mm width. A full ground plane is printed on the antenna backside. To verify the designed approaches, a 3×3 single-port antenna is fabricated, as illustrated in Fig. 13. Following the formerly fabrication process, an end launch connector (number: 1092-03A-5) manufactured by Southwest Microwave is fixed firmly to the antenna feedline.

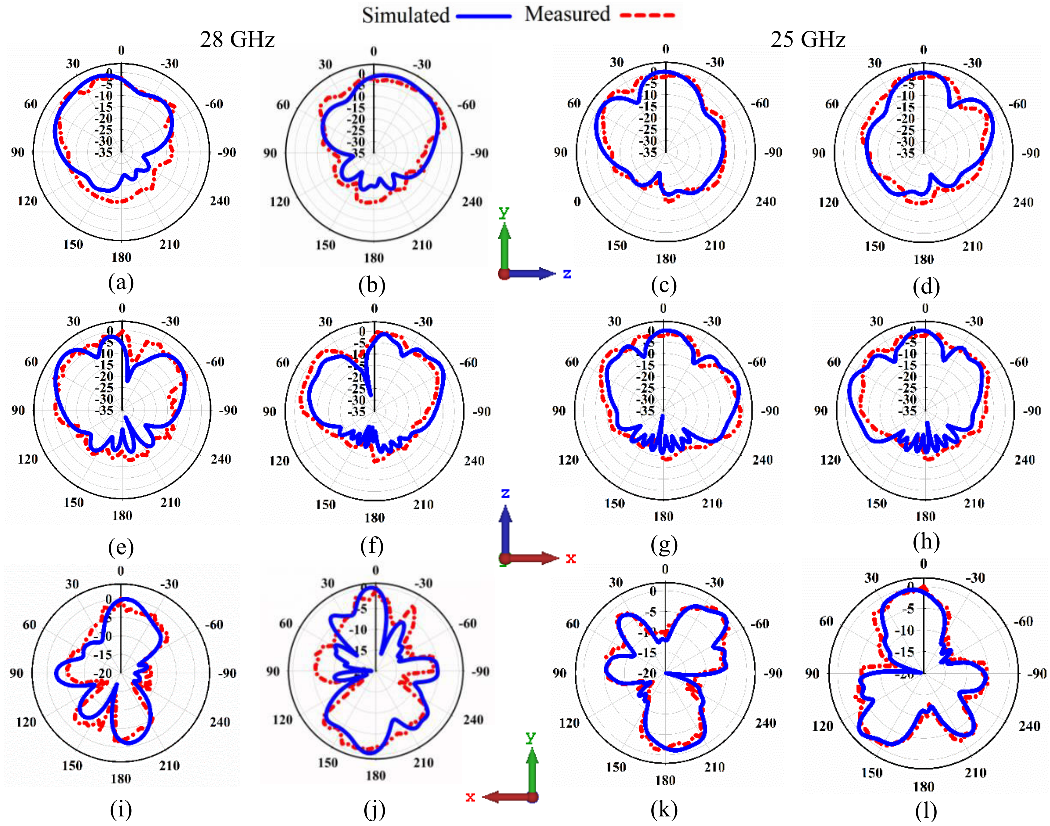

FIGURE 24. Simulated and measured 2D rad. patterns for the MIMO antenna at 28 GHz for planes (a,c) YZ (Ø = 90°) for port 1, (b,d) YZ (Ø = 90°) for port 2, (e,g) XZ (Ø = 0°) for port 1, (f,h) XZ (Ø = 0°) for port 2, (i,k) XY ($\theta = 90°$) for port 1, and (j,l) XY ($\theta = 90°$) for port 2.

B. MIMO ANTENNA

An array of 3×6 MTM patches MIMO antenna (see Fig. 14) is built on a two-layer printed circuit board (PCB), whereas two feeding ports are placed on the opposite side to each other with a 180° angle to enhance the isolation. Fig. 15 depicts the fabricated MIMO antenna prototype to validate the outcomes. A useful technique for ECC calculation is recently introduced by [28] for j^{th} and i^{th} elements of antenna array, respectively. As seen in (1), the ECC will be used based on the 3D far-field radiation pattern method:

$$\rho_{ij}(e) = \frac{\left| \iint_{4\pi} d\Omega \vec{F}_i(\theta,\phi) \times \vec{F}_j(\theta,\phi) \right|^2}{\iint_{4\pi} d\Omega \left| \vec{F}_i(\theta,\phi) \right|^2 . \iint_{4\pi} d\Omega \left| \vec{F}_j(\theta,\phi) \right|^2} \quad (1)$$

where $\vec{F}_i(\theta,\phi)$ and $\vec{F}_j(\theta,\phi)$ are two radiating antenna elements far field property with respect to θ.

V. RESULTS AND DISCUSSION

To provide an understanding of the suggested MIMO antenna working principle, an analysis of the simulated current distribution is indicated. The effects of the MTM structure can be verified by displaying the surface currents of the antenna at 27 GHz and 28 GHz to attain band rejection, as demonstrated in Fig. 15. It is obviously seen that currents surface are mostly intensified surround the edges of inner and outer MTM-shape while the radiation from different sides will be cancelled by each other due to the opposite directions of surface currents along the edges. Fig. 16 shows that the effectiveness of isolation, as when Port 1 is excited, the current distribution will not flow to the Port 2 and vis versa while 50 Ω impedance has been used to terminate the other port.

The backscattered signal (S11) of the suggested single-port antenna in both measured and simulated results is depicted in Fig. 17, with impedance matching better than –10 dB over 24–29.9 GHz, referred to the provided simulation, which covers the future 5G systems at 28 GHz resonance band. The realized S11, S22, S21, and S12 parameters in both simulation and experiment cases of the suggested MIMO antenna based MTM are depicted in Fig. 18.

Good performance is fairly achieved by indicating isolation under quite a low level while varying the location of the antenna element. The minimum bandwidth obtained for S11 is approximately 5.1 GHz with less than -10 dB. It also shows that the maximum realized isolation is below -24 dB in the region of interest. Fig. 19. shows the S-parameters measurement setup for the suggested antenna. Two-elements of the antenna meet the condition of obtaining diversity gain as a very low envelope correlation coefficient is gained and remains below 0.0013, as evident from Fig. 20, which shows a simulated and measured graph of ECC as a function of the frequency between ports 2 and 1. Moreover, the measured and simulated MIMO system diversity gain (DG) is around 9.99 dB at 28 GHz.

The performance of the mm-Wave two-port MIMO antenna systems evaluated by TARC, ECC, and CCL.

These performance parameters are extracted by using the Equations (1) for ECC, (2 and 3) for CCL and TARC [29]. In mm-wave applications, the values of TARC, CCL, and ECC should be lower than 0 dB, 0.5 bits/s/Hz, and 0.5, respectively, for an efficient system of MIMO antenna [29]–[31].

$$CCL = -log_2 det \begin{bmatrix} \alpha_{11} & \alpha_{12} \\ \alpha_{21} & \alpha_{22} \end{bmatrix} \quad (2)$$

where j and i = 1, 2

$$\alpha_{ii} = 1 - \left| \sum_{n=1}^{n=2} S_{in}^{*} S_{ni} \right| \quad and \ \alpha_{ij} = - \left| \sum_{n=1}^{n=2} S_{in}^{*} S_{nj} \right| \quad (2a)$$

$$TARC = \sqrt{\frac{\left|(S_{11} + S_{12}e^{j\theta})\right|^2 + \left|(S_{21} + S_{22}e^{j\theta})\right|^2}{2}} \quad (3)$$

The realized gain is shown in Fig. 21, where its peak values over the achieved operating frequency band make the suggested antenna applicable for 5G communication. The prototype measured peak gain is 12.4 dBi at 28 GHz as calculated after measurements in an anechoic chamber using a well-defined two horn antennas as a reference receiver antenna and transmitter antenna. Besides, the simulated total and radiation efficiencies vary from 88 % to 97 % and 96 % to 98%, respectively, as demonstrated in Fig. 21. Measured and simulated TARC and CCL are portrayed in Figs. 22 (a) and (b). For the proposed two-port metamaterial MIMO configuration, TARC and CCL values are lower than, −7 dB and 0.42 bits/s/Hz, respectively.

The proposed antenna's measurement set up of the radiation pattern is illustrated in Fig. 23. Table 1 presents a comparison of the investigated MIMO antenna based MTM with other reported antenna designs published recently. The MIMO antenna measured and simulated 2D radiation patterns are carried out into E-plane at yz direction and xz direction within phi = (90°, 0°) and xy direction (H-plane) within theta = 90°, as shown in Fig. 24. The far-field properties show excellent directional broadside main beam at yz and xz planes with a certain tilt at 28GHz due to very close placement of array elements, when port 1 is excited, the other elements will be occupied as a reflector. However, from the theta 90° the pattern demonstrates a radiating directive beam towards the direction between xy axis plane when the right or left port is excited. It is clearly indicated that complementary radiation patterns of the ports are occurred to prove the presence of pattern diversity.

VI. CONCLUSION

A low profile millimeter-wave metamaterial-based MIMO antenna array has been suggested for future 5G communication systems, consisting of two ports, each has 3 × 3 array MTM unit cells. The design evolution with performance analysis of MTM, and both single antenna, and MIMO antenna has been analyzed and described. Results demonstrate that the proposed low-profile MTM design exhibited a wide range and effectiveness of near zero for permittivity, permeability, and refractive index characteristics. High isolation >24 dB between MIMO antenna ports is achieved over wide impedance bandwidth from 24 to beyond 30 GHz with low envelope correlation coefficient (ECC) values <0.0013 over the whole operational band. Besides, measured peak gain with 12.4 dBi at 28 GHz, more than 98% efficiency is attained with an overall size of 52 mm × 23 mm. The measured and simulated results are in high agreement, whereas satisfactory performance makes the proposed MTM MIMO antenna appropriate for upcoming 5G networks.

REFERENCES

[1] J. G. Andrews, S. Buzzi, W. Choi, S. V. Hanly, A. Lozano, A. C. K. Soong, and J. C. Zhang, "What will 5G be?" *IEEE J. Sel. Areas Commun.*, vol. 32, no. 6, pp. 1065–1082, Jun. 2014.
[2] M. L. Attiah, A. Isa, Z. Zakaria, M. Abdulhameed, M. K. Mohsen, and I. Ali, "A survey of mmWave user association mechanisms and spectrum sharing approaches: An overview, open issues and challenges, future research trends," *Wireless Netw.*, vol. 26, no. 4, pp. 2487–2514, 2020.
[3] T. S. Rappaport, Y. Xing, G. R. MacCartney, A. F. Molisch, E. Mellios, and J. Zhang, "Overview of millimeter wave communications for fifth-generation (5G) wireless networks—With a focus on propagation models," *IEEE Trans. Antennas Propag.*, vol. 65, no. 12, pp. 6213–6230, Dec. 2017.
[4] Y. Zhang, J.-Y. Deng, M.-J. Li, D. Sun, and L.-X. Guo, "A MIMO dielectric resonator antenna with improved isolation for 5G mm-wave applications," *IEEE Antennas Wireless Propag. Lett.*, vol. 18, no. 4, pp. 747–751, Apr. 2019.
[5] A. Mchbal, N. Amar Touhami, H. Elftouh, and A. Dkiouak, "Mutual coupling reduction using a protruded ground branch structure in a compact UWB owl-shaped MIMO antenna," *Int. J. Antennas Propag.*, vol. 2018, pp. 1–10, Sep. 2018.
[6] F. Wang, Z. Duan, X. Wang, Q. Zhou, and Y. Gong, "High isolation millimeter-wave wideband MIMO antenna for 5G communication," *Int. J. Antennas Propag.*, vol. 2019, pp. 1–12, May 2019.
[7] A. Abdalrazik, A. S. A. El-Hameed, and A. B. Abdel-Rahman, "A three-port MIMO dielectric resonator antenna using decoupled modes," *IEEE Antennas Wireless Propag. Lett.*, vol. 16, pp. 3104–3107, 2017.
[8] L. Zou, D. Abbott, and C. Fumeaux, "Omnidirectional cylindrical dielectric resonator antenna with dual polarization," *IEEE Antennas Wireless Propag. Lett.*, vol. 11, pp. 515–518, 2012.
[9] F. H. Lin and Z. N. Chen, "Low-profile wideband metasurface antennas using characteristic mode analysis," *IEEE Trans. Antennas Propag.*, vol. 65, no. 4, pp. 1706–1713, Apr. 2017.
[10] T. Li and Z. N. Chen, "A dual-band metasurface antenna using characteristic mode analysis," *IEEE Trans. Antennas Propag.*, vol. 66, no. 10, pp. 5620–5624, Oct. 2018.
[11] R. Karimian, A. Kesavan, M. Nedil, and T. A. Denidni, "Low-mutual-coupling 60-GHz MIMO antenna system with frequency selective surface wall," *IEEE Antennas Wireless Propag. Lett.*, vol. 16, pp. 373–376, 2017.
[12] Y. Lee, D. Ga, and J. Choi, "Design of a MIMO antenna with improved isolation using MNG metamaterial," *Int. J. Antennas Propag.*, vol. 2012, pp. 1–7, Jul. 2012.
[13] S. D. Assimonis, T. V. Yioultsis, and C. S. Antonopoulos, "Design and optimization of uniplanar EBG structures for low profile antenna applications and mutual coupling reduction," *IEEE Trans. Antennas Propag.*, vol. 60, no. 10, pp. 4944–4949, Oct. 2012.
[14] Q.-L. Zhang, Y.-T. Jin, J.-Q. Feng, X. Lv, and L.-M. Si, "Mutual coupling reduction of microstrip antenna array using metamaterial absorber," in *IEEE MTT-S Int. Microw. Symp. Dig. Ser. Adv. Mater. Processes RF THz Appl. (IMWS-AMP)*, Jul. 2015, pp. 1–3.
[15] M. Farahani, J. Pourahmadazar, M. Akbari, M. Nedil, A. R. Sebak, and T. A. Denidni, "Mutual coupling reduction in millimeter-wave MIMO antenna array using a metamaterial polarization-rotator wall," *IEEE Antennas Wireless Propag. Lett.*, vol. 16, pp. 2324–2327, 2017.
[16] S. F. Jilani and A. Alomainy, "A multiband millimeter-wave 2-D array based on enhanced franklin antenna for 5G wireless systems," *IEEE Antennas Wireless Propag. Lett.*, vol. 16, pp. 2983–2986, 2017.

[17] S. S. Al-Bawri, M. S. Islam, H. Y. Wong, M. F. Jamlos, A. Narbudowicz, M. Jusoh, T. Sabapathy, and M. T. Islam, "Metamaterial cell-based superstrate towards bandwidth and gain enhancement of quad-band CPW-fed antenna for wireless applications," *Sensors*, vol. 20, no. 2, p. 457, Jan. 2020.
[18] N. Misran, S. H. Yusop, M. T. Islam, and M. Y. Ismail, "Analysis of parameterization substrate thickness and permittivity for concentric split ring square reflectarray element," *J. Kejuruteraan (J. Eng.)*, vol. 23, pp. 11–16, Nov. 2012.
[19] S. S. Islam, M. R. I. Faruque, and M. T. Islam, "A new direct retrieval method of refractive index for the metamaterial," *Current Sci.*, vol. 109, no. 2, pp. 337–342, Jul. 2015.
[20] R. Azim, M. T. Islam, and N. Misran, "A planar monopole antenna for UWB applications," *Int. Rev. Electr. Eng.*, vol. 5, no. 4, pp. 1848–1852, 2010.
[21] M. A. W. Nordin, M. T. Islam, and N. Misran, "Design of a compact ultra-wideband metamaterial antenna based on the modified split-ring resonator and capacitively loaded strips unit cell," *Prog. Electromagn. Res.*, vol. 136, pp. 157–173, 2013.
[22] S. S. Al-Bawri, H. Hwang Goh, M. S. Islam, H. Y. Wong, M. F. Jamlos, A. Narbudowicz, M. Jusoh, T. Sabapathy, R. Khan, and M. T. Islam, "Compact ultra-wideband monopole antenna loaded with metamaterial," *Sensors*, vol. 20, no. 3, p. 796, Jan. 2020.
[23] M. S. Alam, M. T. Islam, and N. Misran, "A novel compact split ring slotted electromagnetic bandgap structure for microstrip patch antenna performance enhancement," *Prog. Electromagn. Res.*, vol. 130, pp. 389–409, 2012.
[24] T. Alam, M. T. Islam, and M. Cho, "Near-zero metamaterial inspired UHF antenna for nanosatellite communication system," *Sci. Rep.*, vol. 9, no. 1, pp. 1–15, Dec. 2019.
[25] A. M. Tamim, M. R. I. Faruque, M. J. Alam, S. S. Islam, and M. T. Islam, "Split ring resonator loaded horizontally inverse double L-shaped metamaterial for C-, X- and ku-band microwave applications," *Results Phys.*, vol. 12, pp. 2112–2122, Mar. 2019.
[26] M. Ullah, M. Islam, and M. Faruque, "A near-zero refractive index meta-surface structure for antenna performance improvement," *Materials*, vol. 6, no. 11, pp. 5058–5068, Nov. 2013.
[27] X. Chen, T. M. Grzegorczyk, B.-I. Wu, J. Pacheco, and J. A. Kong, "Robust method to retrieve the constitutive effective parameters of metamaterials," *Phys. Rev. E, Stat. Phys. Plasmas Fluids Relat. Interdiscip. Top.*, vol. 70, no. 1, Jul. 2004, Art. no. 016608.
[28] M. S. Sharawi, A. T. Hassan, and M. U. Khan, "Correlation coefficient calculations for MIMO antenna systems: A comparative study," *Int. J. Microw. Wireless Technol.*, vol. 9, no. 10, pp. 1991–2004, Dec. 2017.
[29] T. Shabbir, M. T. Islam, S. S. Al-Bawri, R. W. Aldhaheri, K. H. Alharbi, A. J. Aljohani, and R. Saleem, "16-port non-planar MIMO antenna system with near-zero-index (NZI) metamaterial decoupling structure for 5G applications," *IEEE Access*, vol. 8, pp. 157946–157958, 2020.
[30] F. Amin, R. Saleem, T. Shabbir, S. U. Rehman, M. Bilal, and M. F. Shafique, "A compact quad-element UWB-MIMO antenna system with parasitic decoupling mechanism," *Appl. Sci.*, vol. 9, no. 11, p. 2371, Jun. 2019.
[31] T. Shabbir, R. Saleem, S. S. Al-Bawri, M. F. Shafique, and M. T. Islam, "Eight-port metamaterial loaded UWB-MIMO antenna system for 3D system-in-package applications," *IEEE Access*, vol. 8, pp. 106982–106992, 2020.
[32] Y. M. Pan, X. Qin, Y. X. Sun, and S. Y. Zheng, "A simple decoupling method for 5G millimeter-wave MIMO dielectric resonator antennas," *IEEE Trans. Antennas Propag.*, vol. 67, no. 4, pp. 2224–2234, Apr. 2019.
[33] B. Feng, X. He, J.-C. Cheng, and C.-Y.-D. Sim, "Dual-wideband dual-polarized metasurface antenna array for the 5G millimeter wave communications based on characteristic mode theory," *IEEE Access*, vol. 8, pp. 21589–21601, 2020.
[34] A. A. R. Saad and H. A. Mohamed, "Printed millimeter-wave MIMO-based slot antenna arrays for 5G networks," *AEU-Int. J. Electron. Commun.*, vol. 99, pp. 59–69, Feb. 2019.
[35] R. Chandel, A. K. Gautam, and K. Rambabu, "Tapered fed compact UWB MIMO-diversity antenna with dual band-notched characteristics," *IEEE Trans. Antennas Propag.*, vol. 66, no. 4, pp. 1677–1684, Apr. 2018.
[36] M. S. Sharawi, S. K. Podilchak, M. T. Hussain, and Y. M. M. Antar, "Dielectric resonator based MIMO antenna system enabling millimetre-wave mobile devices," *IET Microw., Antennas Propag.*, vol. 11, no. 2, pp. 287–293, Jan. 2017.
[37] N. Jaglan, S. D. Gupta, E. Thakur, D. Kumar, B. K. Kanaujia, and S. Srivastava, "Triple band notched mushroom and uniplanar EBG structures based UWB MIMO/diversity antenna with enhanced wide band isolation," *AEU-Int. J. Electron. Commun.*, vol. 90, pp. 36–44, Jun. 2018.
[38] F. Wang, Z. Duan, Q. Li, Y. Wei, and Y. Gong, "Compact wideband MIMO antenna for 5G communication," in *Proc. IEEE Int. Symp. Antennas Propag. USNC/URSI Nat. Radio Sci. Meeting*, Jul. 2017, pp. 939–940.

SAMIR SALEM AL-BAWRI (Member, IEEE) received the Master of Science degree in wireless communication engineering from Yarmouk University, Jordan, in 2009, and the Doctor of Philosophy degree in communication engineering from Universiti Malaysia Perlis (UniMAP), Malaysia, in 2018. From December 2009 to August 2014, he was a Lecturer with the Faculty of Engineering and Petroleum, Hadhramout University (HU), Yemen. From 2015 to 2018, he was a Graduate Research Assistant with UniMAP. He was a Postdoctoral Researcher Fellow with Multimedia University (MMU), Cyberjaya, Malaysia, for a period of one year. He is currently affiliated with the Center for Space Science, Institut Perubahan Iklim, Universiti Kebangsaan Malaysia (UKM). He has authored or coauthored over fifteen ISI & SCOPUS published journal and nineteen conference proceeding. He is also working toward the 1st patent. His research interests include design and evaluation of multi-element antennas, metamaterials, electromagnetic radiation analysis, localization estimation techniques, and wireless propagation. He was a recipient of the Gold Medal Award at the Breakthrough Invention, Innovation & Design Exhibition Biide2019—UiTM. He also serves as the Editor Manager for the *International Journal of Multidisciplinary Sciences and Advanced Technology* (IJMSAT).

MOHAMMAD TARIQUL ISLAM (Senior Member, IEEE) is currently a Professor with the Department of Electrical, Electronic and Systems Engineering, Universiti Kebangsaan Malaysia (UKM). He is also a Visiting Professor with the Kyushu Institute of Technology, Japan. He has supervised about 30 Ph.D. theses, 20 M.Sc. theses, and has mentored more than ten Postdoctorals and Visiting scholars. He is the author and coauthor of about 500 research journal articles, nearly 175 conference articles, and a few book chapters on various topics related to antennas, metamaterials, and microwave imaging with 22 inventory patents filed. His publications have been cited 6200 times and his H-index is 38 (Source: Scopus). His Google scholar citation is 9200 and H-index is 45. His research interests include communication antenna design, metamaterial, satellite antennas, and microwave imaging. He has been serving as an Executive Committee Member for the IEEE AP/MTT/EMC Malaysia Chapter, since 2018, the Chartered Professional Engineer (CEng), a fellow of IET, U.K., and a Senior Member of IEICE, Japan. He was a recipient of more than 40 research grants from the Malaysian Ministry of Science, Technology and Innovation, Ministry of Education, UKM research grant, international research grants from Japan and Saudi Arabia. He was a recipient of 2018 and 2019 IEEE AP/MTT/EMC Malaysia Chapter, Excellent Award, the Publication Award from Malaysian Space Agency, in 2014, 2013, 2010, and 2009, and the Best Paper Presentation Award, in 2012, the International Symposium on Antennas and Propagation (ISAP 2012) at Nagoya, Japan, and IconSpace, in 2015. He received several International Gold Medal awards, a Best Invention in Telecommunication Award for his research and innovation, and best researcher awards at UKM, in 2010 and 2011, Best Innovation Award, in 2011, and the Best Research Group in ICT niche by UKM, in 2014. He was an Associate Editor of *IET Electronics Letter* and IEEE Access. He serves as the Guest Editor for *Sensors* journal.

TAYYAB SHABBIR received the B.S. degree in electrical (telecommunication) engineering from the COMSATS Institute of Information Technology (CIIT), Islamabad, Pakistan, in 2011, and the master's degree in telecommunication engineering and the Ph.D. degree in antennas and electromagnetics from the University of Engineering and Technology (UET) Taxila, Pakistan, in 2014 and 2019, respectively. Since 2019, he has been Postdoctoral Researcher with the Department of Electrical, Electronic and Systems Engineering, Universiti Kebangsaan Malaysia (UKM), Malaysia. He has published papers in many reputable scientific journals and conferences. His current research interests include UWB-MIMO systems, high gain portable devices, frequency selective surfaces, and reflectarrays. He was a recipient of a fully funded scholarship for his master's and Ph.D. degree.

GHULAM MUHAMMAD (Senior Member, IEEE) received the B.S. degree in computer science and engineering from the Bangladesh University of Engineering and Technology, in 1997, and the M.S. degree and the Ph.D. degree in electrical and computer engineering from the Toyohashi University and Technology, Japan, in 2006 and 2003, respectively. He is currently a Full Professor with the Department of Computer Engineering, College of Computer and Information Sciences, King Saud University (KSU), Riyadh, Saudi Arabia. He has supervised more than 15 Ph.D. and master's Theses. He is involved in many research projects as a principal investigator and a co-principal investigator. He has authored or coauthored more than 250 publications, including the IEEE/ACM/Springer/Elsevier journals, and flagship conference papers. He owns two U.S. patents. His research interests include signal processing, machine learning, the IoT, medical signal and image analysis, AI, and biometrics. He was a recipient of the Japan Society for Promotion and Science (JSPS) fellowship from the Ministry of Education, Culture, Sports, Science and Technology, Japan. He received the Best Faculty Award of Computer Engineering Department at KSU, from 2014 to 2015.

MD. SHABIUL ISLAM (Senior Member, IEEE) received the B.Sc. (Hons.) and M.Sc. degrees from the Department of Applied Physics and Electronics, Rajshahi University, Bangladesh, in 1986 and 1985, respectively, the M.Sc. degree (by research) in micro controller based system design from the Department of Electrical, Electronics and System Engineering, Universiti Kebangsaan Malaysia (UKM), Bangi, Malaysia in 1997, and the Ph.D. degree in VLSI design from the Faculty of Engineering (FOE), Multimedia University (MMU), Cyberjaya, Malaysia, in 2008. From 1991 to 1993, he was a Scientific Officer with The Institute of Electronics and Material Science (IEMS), Bangladesh Atomic Energy Commission (BAEC), Saver, Dhaka, Bangladesh. From July 1999 to July 2009, he was a Lecturer with the Faculty of Engineering, MMU. From July 2009 to March 2012, he was a Senior Lecturer with IMEN, UKM. From June 2010 to December 2012, he was an Associate Fellow with the Department of Electrical, Electronics and System Engineering, Faculty of Engineering and Built Environment, UKM. From March 2012 to December 2016, he worked as an Associate Professor with The Institute of Microengineering and Nanoelectronics (IMEN), UKM. From April 2017 to March 2020, he was an Associate Fellow with IMEN, UKM. He is currently a Professor with the Faculty of Engineering, Multimedia University. He is also the Head of the Micro/Nano Electronics System (MiNES) Laboratory, IMEN. His expertise covers a wide range of engineering disciplines, including micro/nano system design, VLSI design, microcontroller based system design, micro-powering harvesting, and digital communication system. He received internal & external research funds for doing his research work at IMEN, UKM, from 2010 to 2016. His research support also partly contributed to the award of the Higher Education Center of Excellence (HiCOE) from the Malaysian government to IMEN recently. He has published 78 ISI & SCOPUS, five research books, one chapter in book, and 90 conference proceeding. He filed one patent. He is a member of the IEEE Circuits and Systems Society, a Member of the Bangladesh Electronics Society, and an Associate Member of Bangladesh Computer Society (AM476).

HIN YONG WONG (Senior Member, IEEE) received the B.Eng. (Hons.) degree from the University of Sussex, U.K., the M.Sc. (Eng) (Hons.) degree from the University of Leeds, U.K., and the Ph.D. degree in electronic and electrical engineering from the University of Glasgow, U.K. He joined Multimedia University (MMU), Cyberjaya, as a Pioneer Staff Member, where he has been a Lecturer with the Faculty of Engineering, since 1999. Since 1999, he has been a Senior Lecturer, an Associate Professor with the Research Institute Digital Enterprise, where he is currently a Professor and the Director. He was the Dean of the Faculty of Engineering for almost eight years overseeing more than 120 staff and 15 engineering bachelor's and master's programmes. During his tenure as the Dean, he is proud to witness the growth of the faculty from strength to strength. Some of the notable achievements were full accreditation was granted for all the engineering programmes under his care, development of new postgraduate engineering programmes, high number of staff with professional engineers and equivalent qualification for all programmes, the establishment of Graduate Institute of Engineering, average graduate employability of the engineering graduates of above 97%, MMU being ranked Top 200 in the World by QS Working ranking exercise for the discipline of Electrical and Electronic Engineering and many more he has witness He is also supervising/co-supervising over 30 Ph.D. and master's students where many of them have successfully graduated, completed thesis and on thesis writing up stages. He has published book chapter, review chapter, encyclopedia, and 100 international research articles in renowned ISI and Scopus indexed journals and conferences based on his research findings. He has successfully secured a total research grant of over RM 4.9 million for his research projects from various external funding sources His expertise covers wireless communication, semiconductor, nanotechnology, photonics and renewable energy. His research expertise established has resulted in invitations to provide consultancy services to many multi-national companies and wafer foundries. He was a recipient to many prestigious scholastic awards, such the U.K. Tetley & Lupton Scholarship Award, the Overseas Research Students (ORS) Awards, U.K., and the University of Glasgow Postgraduate Research Scholarship awards.